ELSEVIER

Tectonophysics 347 (2002) 231–251

TECTONOPHYSICS

www.elsevier.com/locate/tecto

# Age of the Corsica–Sardinia rotation and Liguro–Provençal Basin spreading: new paleomagnetic and Ar/Ar evidence

F. Speranza [a,*], I.M. Villa [b], L. Sagnotti [a], F. Florindo [a], D. Cosentino [c], P. Cipollari [c], M. Mattei [c]

[a] *Istituto Nazionale di Geofisica e Vulcanologia, Via di Vigna Murata 605, 00143 Rome, Italy*
[b] *Isotopengeologie, Erlachstrasse 9a, 3012 Berne, Switzerland*
[c] *Dipartimento di Scienze Geologiche, Università di Roma Tre, Largo S. L. Murialdo 1, 00146 Rome, Italy*

Received 20 July 2001; accepted 14 January 2002

**Abstract**

The age of spreading of the Liguro–Provençal Basin is still poorly constrained due to the lack of boreholes penetrating the whole sedimentary sequence above the oceanic crust and the lack of a clear magnetic anomaly pattern. In the past, a consensus developed over a fast (20.5–19 Ma) spreading event, relying on old paleomagnetic data from Oligo–Miocene Sardinian volcanics showing a drift-related 30° counterclockwise (CCW) rotation. Here we report new paleomagnetic data from a 10-m-thick lower–middle Miocene marine sedimentary sequence from southwestern Sardinia. Ar/Ar dating of two volcanoclastic levels in the lower part of the sequence yields ages of $18.94 \pm 0.13$ and $19.20 \pm 0.12$ Ma (lower–mid Burdigalian). Sedimentary strata below the upper volcanic level document a $23.3 \pm 4.6°$ CCW rotation with respect to Europe, while younger strata rapidly evolve to null rotation values. A recent magnetic overprint can be excluded by several lines of evidence, particularly by the significant difference between the in situ paleomagnetic and geocentric axial dipole (GAD) field directions. In both the rotated and unrotated part of the section, only normal polarity directions were obtained. As the global magnetic polarity time scale (MPTS) documents several geomagnetic reversals in the Burdigalian, a continuous sedimentary record would imply that (unrealistically) the whole documented rotation occurred in few thousands years only. We conclude that the section contains one (or more) hiatus(es), and that the minimum age of the unrotated sediments above the volcanic levels is unconstrained. Typical back-arc basin spreading rates translate to a duration $\geq 3$ Ma for the opening of the Liguro–Provençal Basin. Thus, spreading and rotation of Corsica–Sardinia ended no earlier than 16 Ma (early Langhian). A 16–19 Ma, spreading is corroborated by other evidences, such as the age of the breakup unconformity in Sardinia, the age of igneous rocks dredged west of Corsica, the heat flow in the Liguro–Provençal Basin, and recent paleomagnetic data from Sardinian sediments and volcanics. Since Corsica was still rotating/drifting eastward at 16 Ma, it presumably induced significant shortening to the east, in the Apennine belt. Therefore, the lower Miocene extensional basins in the northern Tyrrhenian Sea and margins can be interpreted as synorogenic "intra-wedge" basins due to the thickening and collapse of the northern Apennine wedge. 

*Keywords:* Paleomagnetism; Corsica–Sardinia; Liguro–Provencal Basin; Back-arc spreading

* Corresponding author.
*E-mail address:* speranza@ingv.it (F. Speranza).

0040-1951/02/$ - see front matter 
PII: S0040-1951(02)00031-8

## 1. Introduction

The Miocene-to-Present evolution of the Mediterranean region is characterized by the fast opening of several back-arc basins, generally floored by oceanic crust, within the framework of the Africa–Eurasia collision and Alpine orogenesis (e.g. Lonergan and White, 1997; Jolivet et al., 1998).

Constraining the age and spreading rate of those basins is an important part to resolve the geodynamic setting of the Africa–Eurasia boundary during Neogene times. In the western Mediterranean, the Liguro–Provençal Basin, a triangular sea located between the Provençal–Catalan coasts and the Corsica–Sardinia block (Fig. 1), opened during Oligo–Miocene times (Burrus, 1984). Basin spreading and simultaneous eastward migration of the adjacent Alpine belt and Corsica–Sardinia–Calabria blocks were likely driven by the eastward retreat of a Ionian/Adriatic slab passively sinking into the mantle (Malinverno and Ryan, 1986). Since the middle–late Miocene, further roll-back of the same slab caused the spreading of the Tyrrhenian Sea, the southeastward drift of the Calabrian block, and the orogenesis of the Apennines (Patacca et al., 1990).

The basin spreading chronology is fairly well known for the Tyrrhenian Sea, where several drillholes (ODP Leg 107) penetrated the entire sedimentary cover and the underlying continental/oceanic crust (Kastens et al., 1986; Mascle et al., 1988; Sartori,

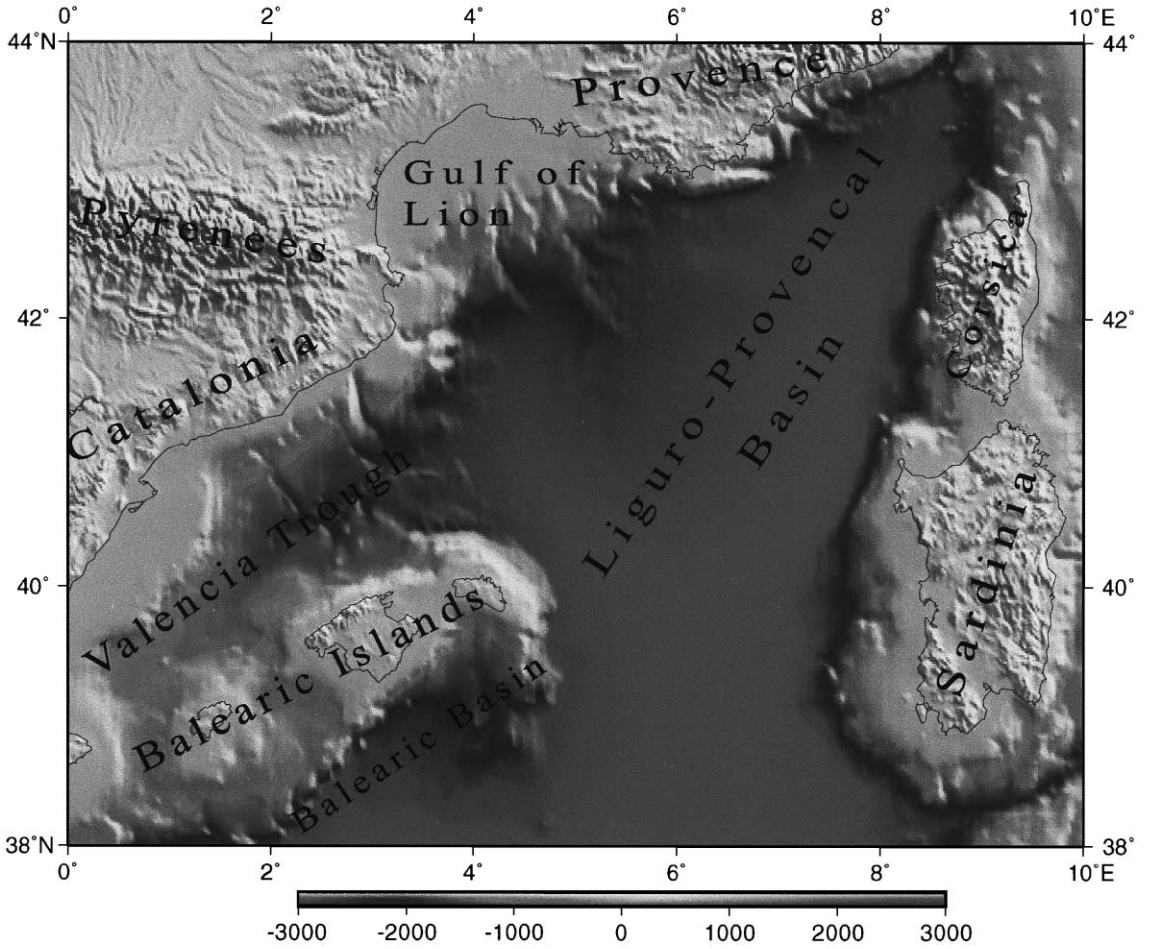


Fig. 1. Shaded relief map of the western Mediterranean Sea and surrounding regions, created by GMT software.

1989). Conversely, borehole data are lacking for the oceanic (and deepest) sector of the Liguro–Provençal Basin. Although the onset of the syn-rift sedimentation is recorded on the Liguro–Provençal conjugate margins (Réhault et al., 1984; Sowerbutts and Underhill, 1998), these data yield age estimates only for the oldest rifting episodes, whereas the drifting age can be constrained only by directly dating the sequences deposited above the oceanic crust.

The Liguro–Provençal spreading took place simultaneously with the eastward drift of the Corsica–Sardinia block, which rotated at least 30° counterclockwise (CCW) about a pole located north of Corsica (e.g. Van der Voo, 1993 and references therein). This drift/rotation link offers the opportunity to indirectly date the Liguro–Provençal opening by means of well-dated paleomagnetic directions. Montigny et al. (1981), by considering K/Ar ages and the synthesis of a large amount of previous paleomagnetic data on the Sardinian volcanics, proposed that the rotation occurred very rapidly between 20.5 and 19 Ma. This hypothesis was widely accepted afterwards, and the paleomagnetic rotation of Sardinia was regarded as a key datum to constrain the Liguro–Provençal spreading age (e.g. Burrus, 1984; Chamot-Rooke et al., 1999). However, a critical analysis of the old paleomagnetic data set based on more modern and stringent criteria demonstrated that coeval paleodeclinations from Sardinia are scattered, hindering a precise definition of the age-related rotation evolution (Todesco and Vigliotti, 1993).

Inconsistencies in the old Sardinian paleomagnetic data likely arise from various sources: (1) few sites are dated, and the ages are obtained through K/Ar dating; (2) a precise tilt correction is almost impossible to perform for most of the calc-alkaline volcanics; (3) the volcanics recorded the directional scatter of the geomagnetic field secular variation; (4) the magnetic mineralogy is complex (as reported by many authors); (5) it cannot be excluded that most of the sites dated at ca. 19 Ma and exhibiting no rotation (and normal magnetic polarity) were recently remagnetized.

In this paper, we report on new paleomagnetic data obtained from a 10-m-thick marine sedimentary section from southwestern Sardinia (Marmilla region). Ar/Ar dating of two volcanoclastic levels from the lower third of the section gives absolute age tie points. The paleomagnetic study of sedimentary strata and the use of Ar/Ar dates allow us to overcome the problems encountered by previous authors, who analyzed volcanic rocks. Our data provide evidence for a post-19 Ma 23° CCW rotation of the Corsica–Sardinia block.

## 2. Age constraints for the Liguro–Provençal Basin spreading

The timing of the Liguro–Provençal Basin spreading has been extrapolated by (1) identification of the pre-, syn- and post-rift sequences in field studies over the basin margins and from offshore seismic reflection data, (2) analysis of the magnetic anomaly pattern in the oceanic crust domain, (3) dating of dredged igneous rocks, (4) dating of calc-alkaline volcanism in western Sardinia, interpreted as the volcanic arc located east of the Liguro–Provençal back-arc basin, and (5) analysis of paleomagnetic data from Corsica and Sardinia (Chamot-Rooke et al., 1999 and references therein).

Extension-related sedimentation is recorded since late Oligocene both in the Catalan–Provençal (Réhault et al., 1984; Mauffret et al., 1992) and Sardinian margins (Assorgia et al., 1997). Although these sediments indicate the first Liguro–Provençal rifting episodes, there is no general consensus on the age of the rift-to-drift transition. In the Valencia trough (Fig. 1), extension continued during the Miocene and Plio–Pleistocene; thus, here, the post-rift sequences cannot be identified (Maillard et al., 1992). Burrus and Foucher (1986), relying on offshore drilling and seismic data, suggest an upper Oligocene–Aquitanian age of the syn-rift sediments and a lower Burdigalian breakup unconformity in the Provençal margin. Onland in western Sardinia, the pre-upper Burdigalian deposits are extensionally faulted, tilted, and unconformably covered by virtually undeformed upper Burdigalian–lower Messinian shallow-marine post-rift successions (Sowerbutts and Underhill, 1998). Lacking deep wells in the central Liguro–Provençal Basin, the strata imaged by seismic reflection data upon the oceanic crust cannot be precisely constrained in age, and are generically referred to the lower–middle Miocene (Burrus, 1984; Mauffret et al., 1992).

The central part of the Liguro–Provençal Basin is characterized by a prominent positive magnetic anomaly (Bayer et al., 1973). This feature is hardly datable

as the correlation to the global magnetic polarity time scale (MPTS) strongly depends on other data sets that can independently constrain the temporal window. Burrus (1984) associated the positive magnetic residuals to the polarity chron C6n (19.048–20.131 Ma according to Cande and Kent, 1995) relying on the approximately 20 Ma age of the Corsica–Sardinia rotation then inferred from paleomagnetic data from Sardinia. This dating has been widely accepted for quite some time, although other authors recently have tended to make the anomaly age younger. Chamot-Rooke et al. (1999) propose that the magnetic anomaly pattern might be more coherently related to anomaly C5Cn, showing a normal polarity triplet in the time interval 16.014–16.726 Ma according to Cande and Kent (1995).

A tristanite sample dredged from a ridge northwest of Corsica yielded an age of $18.0 \pm 0.5$ Ma (Réhault et al., 1984), but recent redating would indicate a $\sim 17$ Ma age (Chamot-Rooke et al., 1999). More recently, several volcanic edifices were sampled northwest and southwest of Corsica, and Ar/Ar and fission tracks dating indicate $16.1 \pm 04$ and about 17.5 Ma ages, respectively (Deverchère, 1996). However, the use of dredged igneous rocks ages to constrain the timing of basin opening remains controversial as (1) the volcanic cones west of Corsica display both arc- and rift-type signature, making unclear whether they are related to the Liguro–Provençal Basin spreading or whether they represent the northern prolongation of the Sardinian volcanic arc, and (2) isolated volcanic eruptions may not be linked to and can occur after, the basin spreading.

In western Sardinia a wealth of calc-alkaline volcanics (mainly domes and ignimbrites) crop out along the N–S Sardinia Trough (Fig. 2) interbedded with upper Oligocene–upper Miocene sediments. Their age (13–32 Ma according to Beccaluva et al., 1985) was used to approximate the time span comprising the whole Liguro–Provençal rifting and drifting events (Vigliotti and Langenheim, 1995). We note, however, that arc volcanism is attributed to the activity of the subduction process beneath Sardinia, which may have continued also after the cessation of the Liguro–Provençal Basin spreading. Therefore, the end of the Liguro–Provençal spreading is not constrained by the cessation of Sardinian calc-alkaline volcanism at 13 Ma.

Since the late 1960s and during the 1970s, several paleomagnetic studies were carried out on the Sardinian rocks (De Jong et al., 1969, 1973; Zijderveld et al., 1970; Coulon et al., 1974; Manzoni, 1974; Edel and Lortscher, 1977; Edel, 1979; Horner and Lowrie, 1981). Mainly the Oligo–Miocene and Permian volcanics were sampled. The data showed two $\sim 30^\circ$ CCW rotation events with respect to Europe occurring during late Mesozoic–early Tertiary and early–middle Miocene times, respectively (e.g. Van der Voo, 1993). The debatable coupling or decoupling between Corsica and Sardinia during drifting (Westphal et al., 1976) was resolved by Vigliotti et al. (1990), who showed that after the Permian the two islands rotated as one block.

The Tertiary paleomagnetic data set was completed and synthesized by Montigny et al. (1981), who proposed the 20.5–19 Ma fast rotational event. More recently, Todesco and Vigliotti (1993) showed that a $30–40^\circ$ scatter in declinations exists among coeval paleomagnetic sites considered by Montigny et al. (1981), and that coeval normal and reverse polarity directions are not antipodal, strongly reducing the reliability of the whole data set. Moreover, after a careful statistical analysis of the existing data, they confirmed a 20–21 Ma age for the beginning of rotation, but showed that the termination of the rotation is virtually unconstrained.

Recently, paleomagnetic data from three Sardinian upper Burdigalian–Langhian sedimentary sites (Vigliotti and Langenheim, 1995) seemed to indicate that at 15–18 Ma, the rotation was not yet completed. Finally, Gattacceca (2001) and Deino et al. (2001) have reported new paleomagnetic data and Ar/Ar ages from volcanics exposed in several central–northern Sardinia localities, also resampling some units studied by Montigny et al. (1981). Their data confirm that Sardinia started rotating at $\sim 21$ Ma, and indicate that the overall rotation was as high as $50^\circ$. A well-constrained tie point in the rotation history further documents that $13^\circ$ of rotation occurred after $18.18 \pm 0.03$ Ma.

## 3. Geological outline of the Marmilla region

The earliest marine deposits of the late Paleogene–Neogene sedimentary cycles in central Sardinia are Chattian in age and belong to the Riu Su Rettore Fm. (Farris, 1990). This latter has been correlated to the

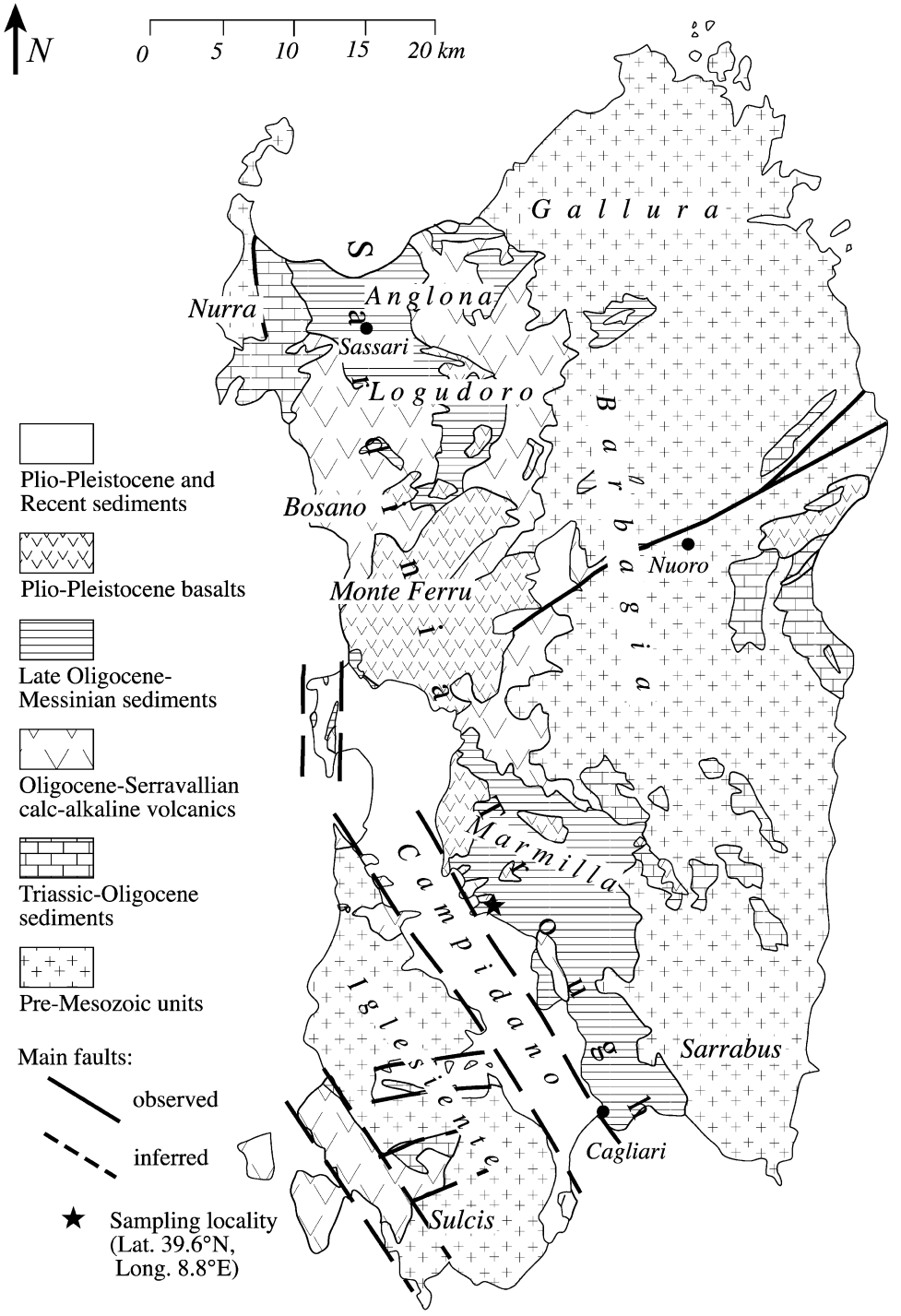


Fig. 2. Simplified geological map of Sardinia and location of the sampling locality.

uppermost part of the Ussana Fm. (Pecorini and Pomesano Cherchi, 1969), late Oligocene–earliest Miocene in age. Despite the older age of these deposits, all over the central and northern Sardinia the marine transgression is widely extended only starting from the earliest Aquitanian (Assorgia et al., 1992a,b, 1997; Barca et al., 1996) when, in western Sardinia, extensional tectonics gave rise to the so-called ''Sardinia Trough''. This is a N–S trending elongate zone where the pre-Mesozoic crystalline rocks are covered by Tertiary continental and marine sediments interbedded with mainly Miocene calc-alkaline volcanics (Fig. 2). Both in the northern Iglesiente (Funtanazza section, Assorgia et al., 1988) and in Marmilla, the basal portion of the marine succession, sedimented above the continental deposits (Ussana Fm. and/or Sa Tellura lacustrine limestones), is referable to the N4 Zone (Blow, 1967).

In the Marmilla region, particularly between Sardara and Villanovaforru villages, the lower portion of the Marmilla Fm. has been referred to the lower Burdigalian by means of calcareous nannofossil assemblages (Iaccarino et al., 1985; Cherchi et al., 1985). In the same area, close to the Collinas village, silicized marly horizons and andesitic lava bodies with frequent pillow structures testify an intense submarine volcanic activity. In this region, the early Miocene sedimentary basin was also affected by strong instability, probably linked to intense syn-sedimentary tectonics. Here, the sedimentary succession shows angular unconformities, channellized coarse-grained deposits and frequent slumped horizons. Moreover, the Lower Miocene deposits (belonging to the 1st Miocene sedimentary cycle) are cut by growth-faults and by faults that are sealed by younger sediments. The instability of the Marmilla sedimentary basin has to be related to the tectonic activity connected with the spreading of the Liguro–Provençal Basin.

The Upper Oligocene–?upper Burdigalian deposits are unconformably overlain by the 2nd Miocene sedimentary cycle (Langhian–?upper Serravallian) through an irregular surface characterised by a stratigraphic gap and, sometimes, by continental deposits (central–southern Sardinia) and/or by calc-alkaline ignimbrites (central-northern Sardinia) (Assorgia et al., 1997). In the Marmilla region, the 2nd Miocene sedimentary cycle is mainly characterised by marly and silty–marly deposits of the Marne di Gesturi Fm.

## 4. Geological features and biostratigraphy of the studied sedimentary section

The studied stratigraphic section has been sampled along a new (in 1995) N–S subvertical road cut, to the NE of the Collinas village (Lat. 39.6°N, Long. 8.8°E, Fig. 2). The section is about 10 m thick. Bed dip is towards the SE and decreases from 22° in the northern (lower) part of the section to 11° in the southern (upper) part. The lower 5.3 m of section are mainly composed by calcareous marls interbedded with conglomeratic levels and by arenaceous and volcaniclastic horizons. In particular, at 1.8 and 3.3 m above the base of the section, we sampled for radiometric dating purposes two yellow volcaniclastic layers (LV1 and LV2), 10 and 25 cm thick, respectively (Fig. 3). They are calc-alkaline volcanic sandstones, mostly consisting of quartz, plagioclase and k-feldspar grains. The calcareous marls are normally blue-grey except above LV1, where they turn into yellow for a thickness of about 40 cm (Fig. 3).

An abrupt lithologic change occurs at about 5.3 m above the base of the section. Here, the marly thick strata pass upwards, through a highly irregular surface (disconformity), to blue-grey clays containing scattered marly strata 10–30 cm thick. The clays are about 4 m thick and pass upwards to a chaotic clayey complex including slumps from marly beds. The marls of the lower part of the section are cut by E–W syn-sedimentary normal faults, producing maximum offsets of some centimeters, which are sealed by the clays.

A biostratigraphic analysis, based on calcareous nannofossil assemblages, has been carried on all the samples collected for paleomagnetic study. Despite the very dense sampling (average spacing of 10 cm), the scarce presence of nannofossils prevented a quantitative analysis. Moreover, strong etching affected the nannofossil assemblage, inducing the preservation exclusively of the more resistant species such as *Dictyococcites* sp., *D. scrippsae*, *D. productus*, *Coccolithus pelagicus*, *Cyclicargolithus floridanus*, *Sphenolithus moriformis*. Unfortunately, these species are not significant from a biostratigraphic point of view. However, samples collected close to the study section, in a lower stratigraphic position, provided more constraining data. Even if also in these samples the assemblages are mainly characterised by very resistant species (*C. pelagicus*, *Dictyococcites* sp., *D. scrippsae*, *D. produc-*

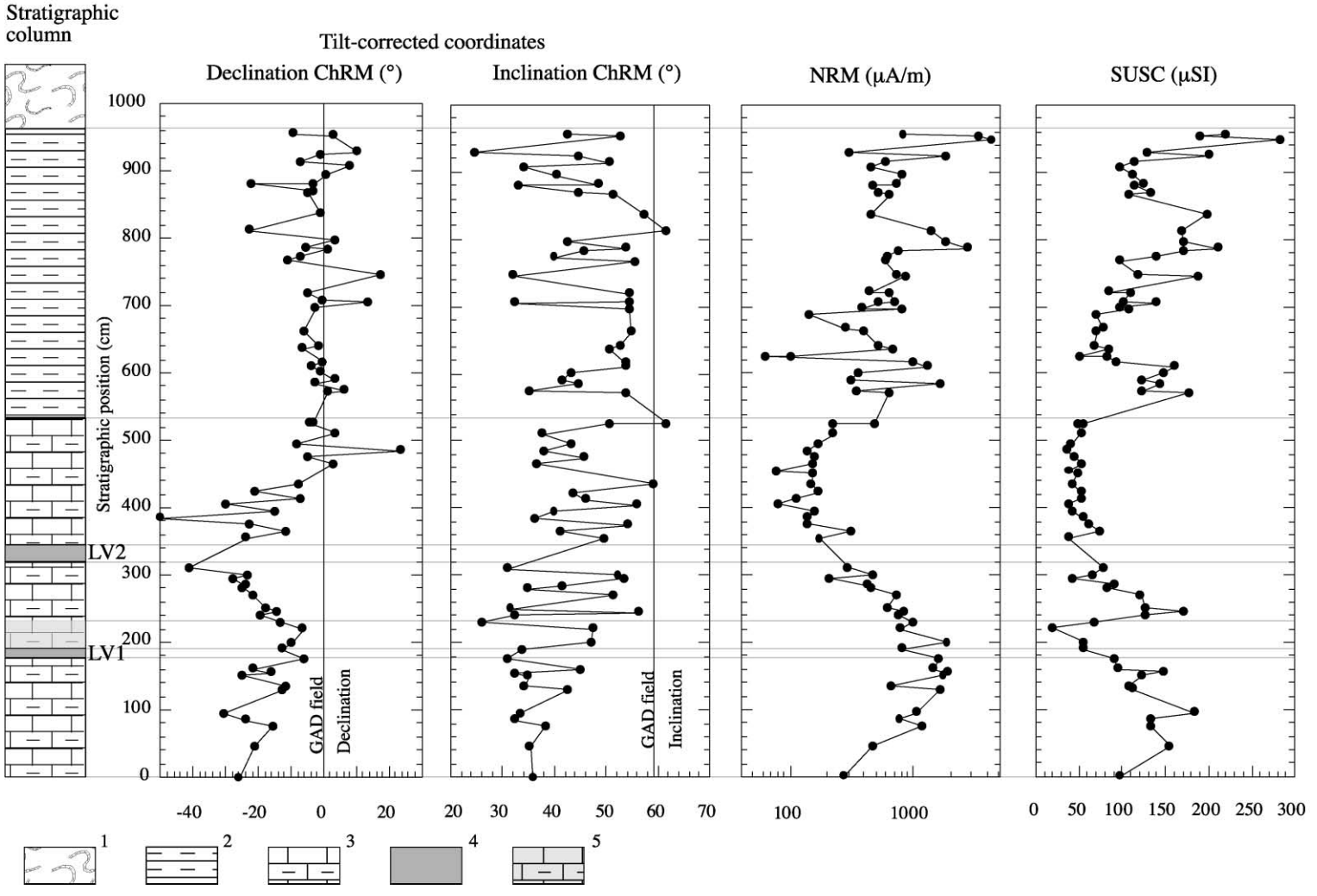


Fig. 3. Stratigraphic column of the studied section and correspondent magnetic parameters. The stratigraphic positions are referred to the bottom of the exposed section. Lithologies: (1) chaotic clayey complex; (2) clays with subordinate marly levels; (3) blue-grey marls; (4) volcanoclastic levels; (5) yellow marls.

*tus, Cy. floridanus*, *S.* gr. *moriformis*), delicate species have been detected (*Helicosphaera carteri* and *Reticulofenestra* < 7 μm). As *H. carteri* is commonly present since the lowermost analyzed samples, this portion of succession can be located above the First Common Occurrence (FCO) of this species and then it should not be older than the top of MNN 1d Zone (Fornaciari and Rio, 1996), which is early Burdigalian. This age is in agreement with the data coming from the biostratigraphic analyses performed on a stratigraphic section of the Marmilla Fm., located a few kilometers to the south of the Collinas area, along the Sardara–Villanovaforru road. In this section, nannofossil assemblages are generally better preserved. The species detected are the same, but they are much more abundant with respect to those of Collinas. Furthermore, previous biostratigraphic analyses, based on planktonic foraminifera, referred the Sardara–Villanovaforru section to the *Catapsidrax dissimilis* Subzone (Iaccarino et al., 1985), confirming an early Burdigalian age.

## 5. Paleomagnetic sampling

We drilled 84 cores along the section (average spacing of 10 cm) using an ASC 280E petrol-powered portable drill, and oriented them in situ using a magnetic compass. We drilled 42 cores in the lower marls (Fig. 3) and avoided the volcanoclastic levels as they likely did not average the secular variation of the geomagnetic field. The remaining 42 cores were sampled from the upper clayey section. As a consequence of the bedding attitude and the road cut orientation, the lower section crops out in the north, whereas the upper beds are mainly exposed in the south. Therefore, we drilled the cores along two vertical profiles, about 25 m apart: 62 samples (from both the lower marls and the upper clays) were drilled in the north (bedding dip here is 22°), while the remaining 22 samples (two from the marls and 20 from the clays) were collected in the south, where the beds dip 11°.

## 6. Anisotropy of magnetic susceptibility

The low-field magnetic susceptibility ($k$) and anisotropy of magnetic susceptibility (AMS) of all the 84 samples was measured with a KLY-2 bridge (Agico) in the paleomagnetic laboratory of the Istituto Nazionale di Geofisica e Vulcanologia (Roma). Susceptibility values are generally < 200 μSI (Fig. 3), then they probably reflect the main contribution of the paramagnetic clay minerals (i.e. Sagnotti et al., 1998). The lowest $k$ values (30–50 μSI) are measured in the marls located between LV2 and the clays, suggesting a reduced input of the terrigenous (clay) fraction at such stratigraphic interval.

The AMS was evaluated using Jelinek (1978) statistics. In almost all samples, the magnetic foliation plane is always well defined and parallel to the bedding plane (Fig. 4), as is commonly observed in undeformed to weakly deformed sediments. Therefore, AMS data show a typical sedimentary fabric and help to exclude both anomalous magnetic fabrics due to peculiar magnetic mineralogy (e.g. Gialanella et al., 1994; Lehman et al., 1996) and significant tectonics-related fabric modification.

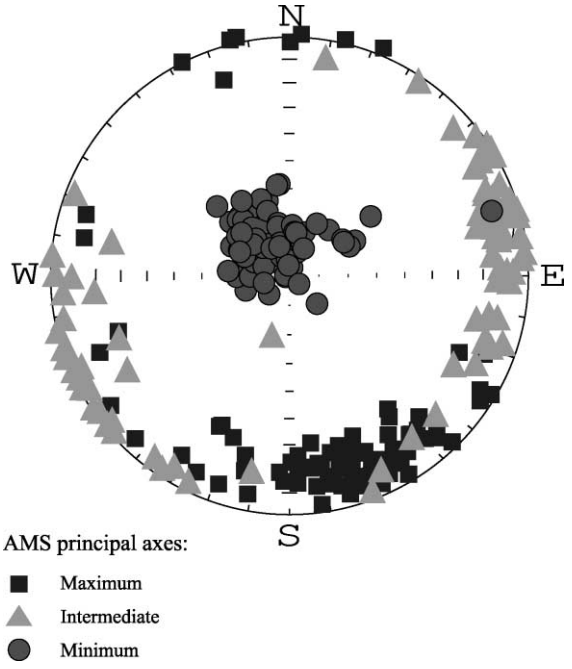


Fig. 4. Anisotropy of magnetic susceptibility (AMS) data for all the samples; Schmidt equal-area projection, lower hemisphere, geographic coordinates. The magnetic foliation (i.e. the plane containing the maximum and intermediate susceptibility axes) of almost all the samples is subparallel to bedding, showing a typical sedimentary fabric.

## 7. Paleomagnetism

The natural remanent magnetization (NRM) of all the 84 samples was measured, and the magnetic mineralogy of 14 representative samples was specifically investigated (about one sample every 65 cm). All the measurements were done in the magnetically shielded room of the paleomagnetic laboratory at the Istituto Nazionale di Geofisica e Vulcanologia.

### *7.1. Magnetic mineralogy*

For the selected 14 specimens, we studied the isothermal remanent magnetization (IRM) acquisition curves up to 900 mT (Fig. 5a) and the coercivity of remanence (Hcr), evaluated by applying an increasing back-field to the IRM at 900 mT (Fig. 5b). The inducing field was imparted stepwise by a 2G pulse magnetizer, and the remanence was measured in-line with a 4.5 cm access pass through 2G cryogenic magnetometer. Seven out of fourteen samples (equally distributed through the section) are virtually saturated at 100–200 mT (samples SA0205B and SA0222B in Fig. 5a), and showed an Hcr ranging from 30 to 50 mT (Fig. 5b). In the remaining samples, the ratio between the remanence acquired at 100 and 900 mT is 60–70%, and the Hcr ranges from 50 to 80 mT. Therefore, in about 50% of the samples, the main magnetic carriers are only low-coercivity minerals, while in the others, both low- and high-coercivity minerals coexist.

In order to better define the nature of these low-coercivity and high-coercivity magnetic fractions, we thermally demagnetized a three-component IRM (acquired at fields of 900, 500 and 120 mT applied in sequence along the three sample axes), according to the method of Lowrie (1990). In the samples containing only the low-coercivity fraction, the magnetization is unblocked between 550 and 600 °C (Fig. 5c), indicating the presence of magnetite. In the specimens sampled in the yellow marls above LV1, a minor amount of high-coercivity fraction (not detected during IRM acquisition) is demagnetized between 600 and 650 °C, showing that some hematite is associated to magnetite (Fig. 5d). In the samples containing a mixture of magnetic minerals, the low-coercivity fraction is demagnetized between 550 and 600 °C (indicating magnetite), while the high-coercivity fraction is unblocked either below 120 °C (Fig. 5e), or between 600 and 650 °C (Fig. 5f), indicating the presence of goethite and hematite, respectively. An intermediate-coercivity phase with maximum unblocking temperatures of 300–400 °C was noticed in most of the samples (Fig 4c–e). Furthermore, in some cases, a low- to intermediate-coercivity phase with unblocking temperature of about 180–220 °C was also observed (Fig. 5f). These magnetic properties are not uniquely linkable to a specific magnetic mineral and may be due to magnetic iron sulphides, maghemite or high-Ti titanomagnetites.

As a summary, the studied samples contain a complex magnetic mixture in which magnetite carries the main part of remanence, but small amounts of goethite, hematite and other magnetic minerals are present.

### *7.2. Demagnetization of the natural remanent magnetization*

The NRM of all the 84 samples (one sample per core) was thermally demagnetized in 10–15 steps (13 in average) and the remanence was measured using a JR-5A spinner magnetometer (Agico). NRM intensities are higher (greater than 500 μA/m) in the marly levels around LV1 and in most of the upper clays, while lower values (between 100 and 200 μA/m) are measured in the marls located between LV2 and the clays (Fig. 3). The magnetization directions from each sample were analyzed in orthogonal diagrams and the characteristic remanence components were evaluated using the principal component analysis (Kirschvink, 1980).

In all the samples, a viscous component subparallel to the present-day field is eliminated by 250 to 310 °C (Fig. 6). In about 60% of the samples, a characteristic remanent magnetization (ChRM) is defined between 250 and 550 °C (Fig. 6a). In four samples from the yellow marls above LV1, two different components are unblocked between 310 and 460 °C [low temperature (LT) component] and 460–600 °C [high temperature (HT) component], respectively (Fig. 6b). As the HT component is subparallel to the present-day field and is likely carried by hematite, it probably arises from recent alteration of magnetite and acquisition of a chemical remanent magnetization by hematite. Therefore, this HT component was not considered to have tectonic implications.

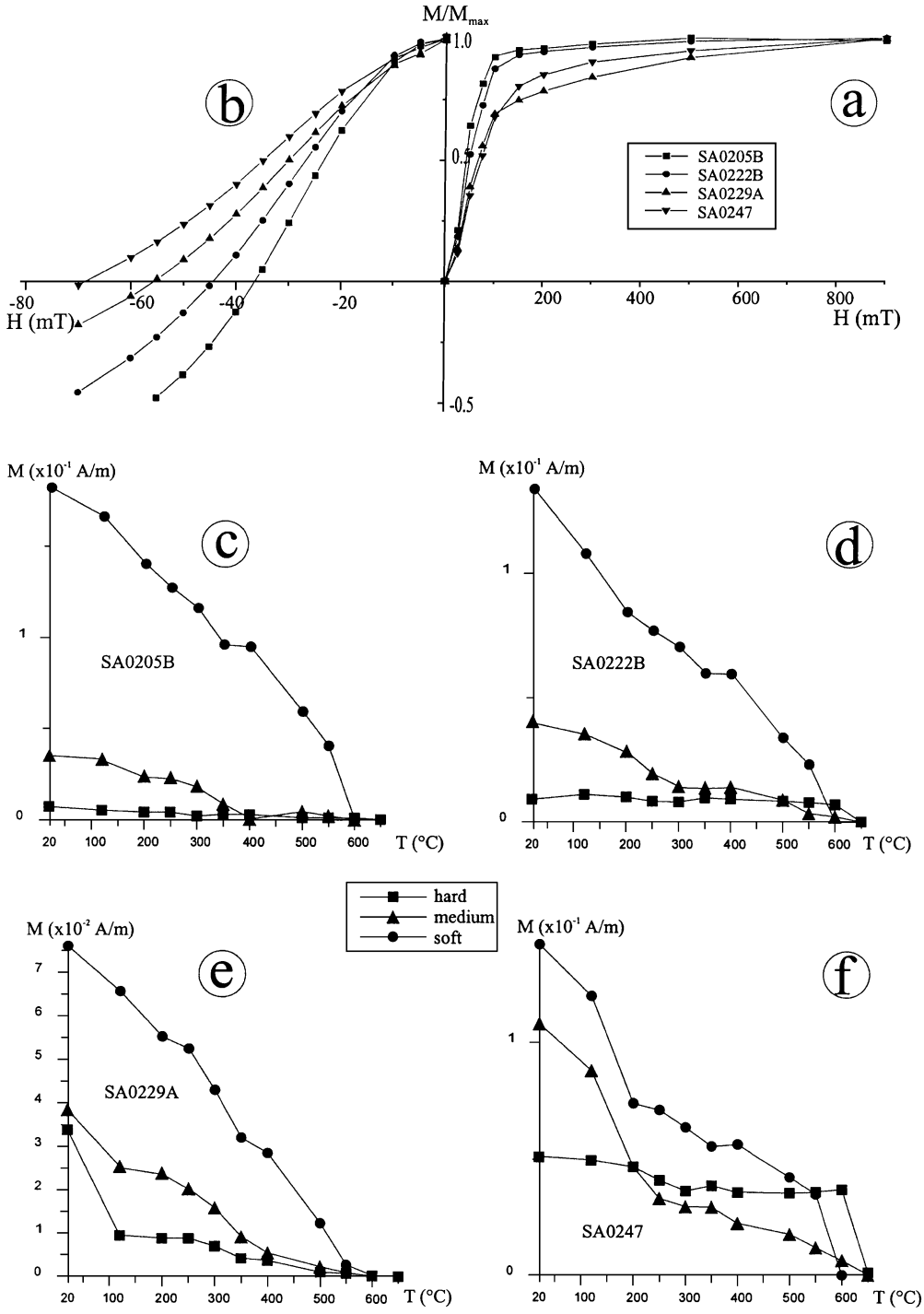
M/M$_{max}$
1.0
0.5
-0.5
b
a
SA0205B
SA0222B
SA0229A
SA0247
-80
-60
-40
-20
200
400
600
800
H (mT)
H (mT)
M (x10$^{-1}$ A/m)
c
SA0205B
T (°C)
M (x10$^{-1}$ A/m)
d
SA0222B
T (°C)
hard
medium
soft
M (x10$^{-2}$ A/m)
e
SA0229A
T (°C)
M (x10$^{-1}$ A/m)
f
SA0247
T (°C)

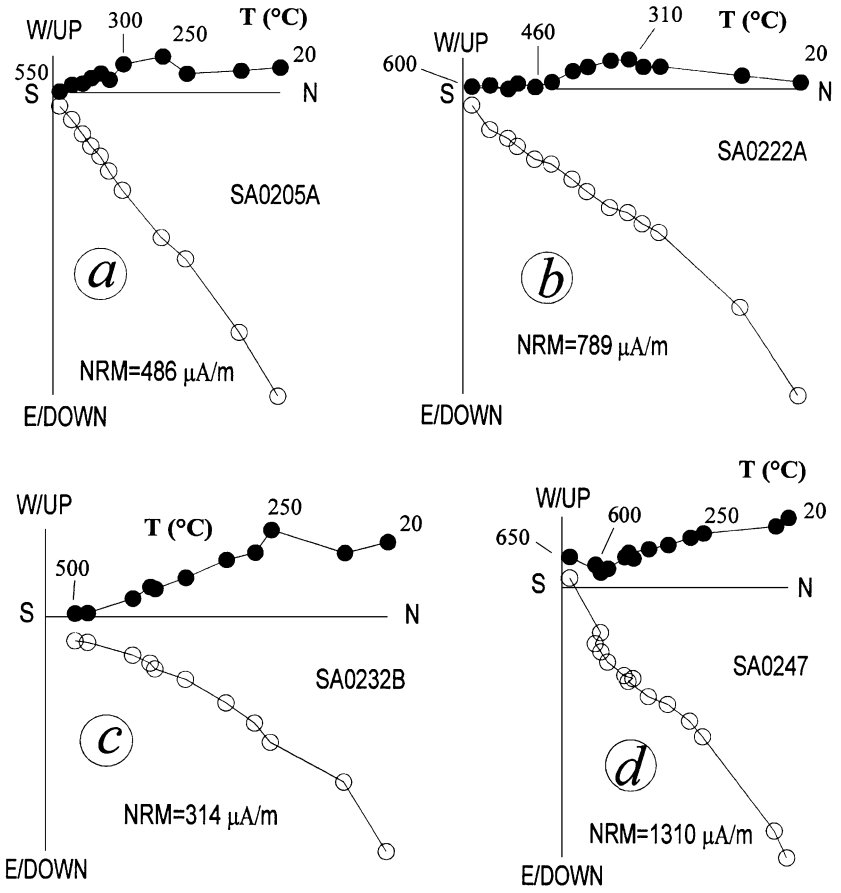


Fig. 6. Vector diagrams of typical thermal demagnetization data, in geographic coordinates. Open and solid symbols represent projections on the vertical and horizontal planes, respectively. All the samples show a viscous component parallel to the present-day field unblocked at 250–310 °C. (a) Sample showing a single magnetization component (after the removal of the viscous component), (b) sample from the yellow marls showing LT and HT components, (c) sample showing a linear decay not anchored to the origin in the interval 250–500 °C, (d) sample showing a well defined ChRM below 600 °C and scattered directions above 600 °C.

In about 30% of the samples, the ChRM is well defined between 250 and 500 °C (Fig. 6c), but the best-fit line does not pass through the origin of the orthogonal diagram, implying that a small (and not resolvable) HT component above 500 °C is also present. In a few samples containing both magnetite and hematite, a characteristic component carrying 85–90% of remanence is well resolvable between 250 and 600 °C, while above 600 °C, scattered directions of magnetization (carried by hematite) are observed (Fig. 6d). Finally, about 10% of the samples (mainly from the upper clays) yielded random changes of the paleomagnetic

Fig. 5. Results of rock magnetic measurements for some representative samples. Acquisition of normalized IRM up to 0.9 T (a), back field demagnetization curve (b), and thermal demagnetization of a three-component IRM according to Lowrie (1990) (c–f). (c) Sample containing prevailing magnetite and an intermediate-coercivity phase with maximum unblocking temperature of ca. 350–400 °C, (d) sample from the yellow marls containing prevailing magnetite, hematite and an intermediate-coercivity phase with maximum unblocking temperature of ca. 250–300 °C, (e) sample containing prevailing magnetite, goethite and an intermediate-coercivity phase with maximum unblocking temperature of ca. 350–400 °C, (f) sample containing magnetite, hematite and a low- to intermediate-coercivity phase with maximum unblocking temperature of ca. 200–250 °C. See text for discussion.

direction during heating and no ChRM could be calculated. Overall, a well-defined ChRM could be isolated for 73 out of 84 samples (Fig. 3).

All the identified remanence components have a normal polarity. This observation, coupled with the recognition of a complex mineral magnetic mixture suggests that the present-day normal component removed at low-temperature may be due to recent remagnetization, whereas we interpret the ChRM component as a primary remanence carried by different detrital minerals (magnetite, maghemite?, titanomagnetite?).

### 7.3. Paleomagnetic directions

The 73 samples revealing reliable paleomagnetic results show normal polarity ChRMs (Fig. 7). Marly samples below LV2 show systematic northwestward declinations (Fig. 3), whereas the samples from the upper clays display on average northward declinations.

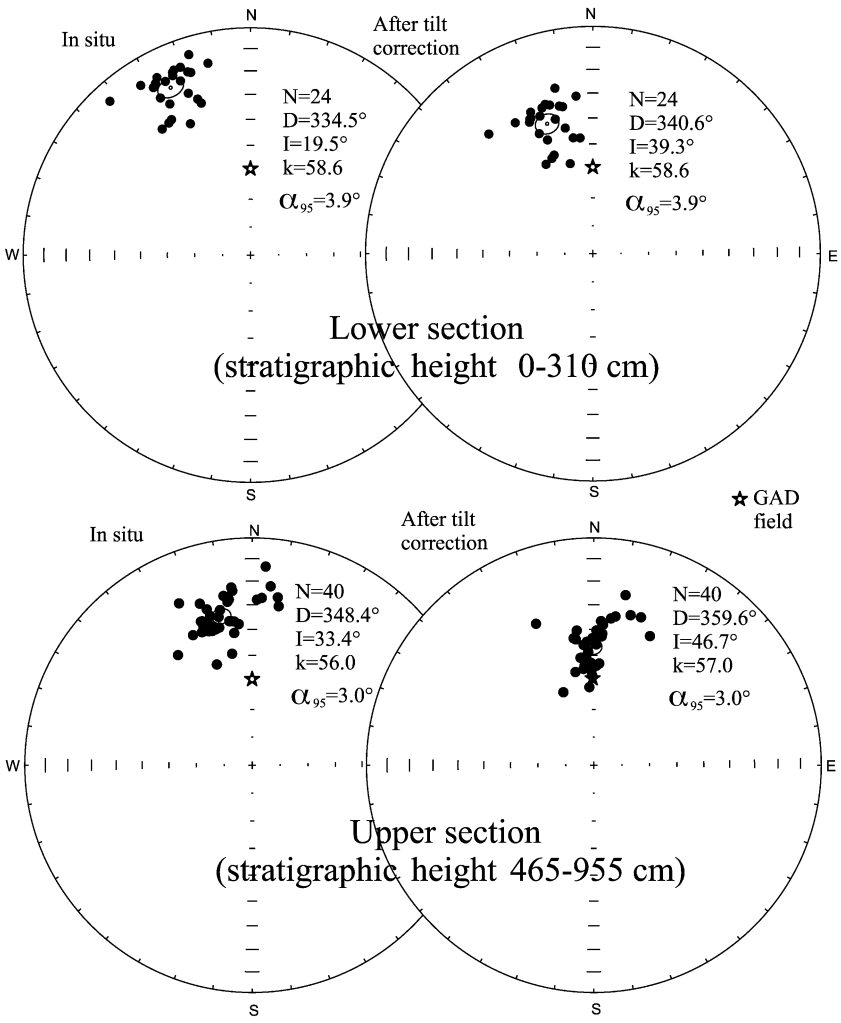


Fig. 7. Equal-area projection (lower hemisphere) of the ChRMs from the studied section. The open circles and ellipses are the projections of the mean paleomagnetic directions and the relative $\alpha_{95}$ cones, respectively. The GAD field direction for the locality (Lat. 39.6°N, Long. 8.8°E) is also represented (stars). Lower section samples are from the marls below LV2, upper section samples are from the upper marls and clays (see also Fig. 3).

The marls located above LV2 show scattered declinations rapidly passing upward from northwestward to northward (on average) directions.

When analyzed separately, the ChRMs from the marls below LV2 and the upper marls/clays define paleomagnetic mean directions, which are significantly different (Fig. 7). After tilt correction, they are defined by $N=24$, $D=340.6°$, $I=39.3°$, $k=58.6$, $\alpha_{95}=3.9°$ for the lower stratigraphic interval (0–310 cm), and $N=40$, $D=359.6°$, $I=46.7°$, $k=57.0$, $\alpha_{95}=3.0°$ for the upper stratigraphic interval (465–955 cm, Fig. 7). Given the slight difference in bedding attitude (11°) observed through the section, the fold test applied to the two intervals (according to McFadden, 1990) is not significant: $\xi_{\text{in situ}}=0.148$; $\xi_{\text{unfolded}}=0.266$; $\xi_{95\%}=7.357$.

There are several bits of evidence suggesting that the isolated ChRM is a primary (post) depositional remanence: (1) The in situ paleomagnetic directions from the whole section are far from the local geocentric axial dipole (GAD) field direction (Fig. 7). (2) The tilt-corrected mean inclinations from the lower ($I=39.3°$) and upper section ($I=46.7°$) are both significantly shallower than both the local GAD field inclination ($I=58.8°$) and the lower–middle Miocene inclination (53.9°) predicted for Europe (Besse and Courtillot, in press), and similar paleomagnetic flattening in sediments are commonly due to compaction-related effects. In fact, AMS data have confirmed the presence of an almost purely sedimentary fabric. (3) The large scatter in inclination values (Fig. 3) suggests a prolonged remanence acquisition (i.e. during sedimentation) rather than a single remagnetization episode that should produce less scattered data (see May et al., 1986). Scatter is not due from inherent noise due to weak remanence since the linear segments of the demagnetization diagrams are well defined (Fig. 6), and inclination scatter is similar in both weakly and strongly magnetized samples (Fig. 3). (4) The presence of a multicomponent ChRM (Figs. 5 and 6) instead of a single overprint-related component.

## 8. Ar/Ar dating of the volcanoclastic levels

Two feldspar separates (one from each volcanoclastic level) were analyzed by $^{39}Ar$–$^{40}Ar$ stepwise heating. Experimental procedures followed Belluso et al. (2000). Age spectra are internally discordant, which means that no "plateau" is formed; however, progress in understanding Ar isotope systematics now allows to obtain robust and reliable ages even in the absence of a "plateau" (e.g. Villa et al., 2000). The Ca/K vs. Cl/K chemical correlation diagram (for a discussion, see Belluso et al., 2000) shows that the separates consist of several (at least three) Ar reservoirs, i.e. intergrown minerals. One low-temperature step showing a high Cl/K ratio is likely to reflect an alteration product (clays or fluid inclusions), as feldspars are known not to incorporate Cl in their structure (Smith, 1974). In all other steps, the Cl/K ratio does not correlate in an obvious way with age.

The Ca/K ratio also correlates very weakly with the apparent age. This is unusual and might point to the fact that the various minerals in the separates are intergrown at the 200-nm scale so that recoil of reactor-produced Ar causes blurring of the isotope ratios.

Isochrons were calculated for all samples. Invariably, they showed excess scatter (high values of the MSWD parameter: Ludwig, 1999), which can be attributed to the presence of several mineral subsystems with different initial $^{40}Ar/^{36}Ar$ ratios. What is more important, however, is that all calculated intercepts of all reasonable subset fits are atmospheric within 1 standard deviation. This means that there is no evidence for an unusual trapped Ar component. In turn,

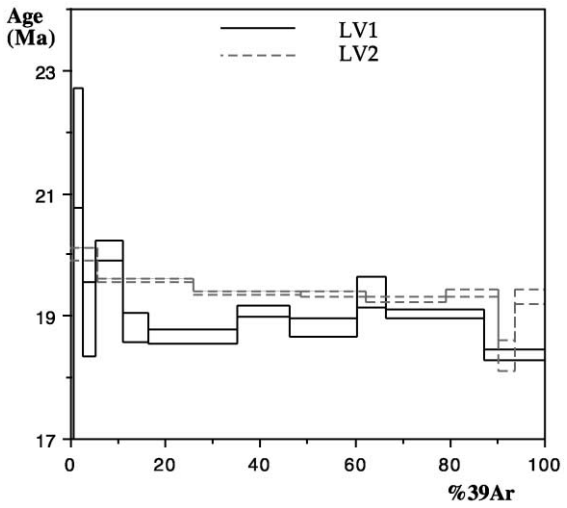


Fig. 8. $^{40}Ar/^{39}Ar$ age spectra of two feldspar separates from the volcanoclastic level LV1 and LV2, respectively.

this gives confidence that estimates based on step ages (calculated assuming an atmospheric trapped Ar, and shown in Fig. 8) are fairly reliable. For both samples, we calculate the weighted average of those steps most likely to correspond to pristine feldspar, i.e. those with lowest Cl/K ratios: for LV1, the six steps having Cl/K < 0.0009 and a uniform Ca/K between 5 and 7 account for 73% of the total Ar and give $t = 18.94 \pm 0.13$ Ma; for LV2, five steps having Cl/K < 0.0006 and Ca/K < 1 account for 85% of the total Ar and give $t = 19.20 \pm 0.12$ Ma. Assuming that the two levels are contemporaneous, their common age is calculated as $19.08 \pm 0.09$ Ma.

## 9. Discussion

### 9.1. Correlation with the global magnetic polarity time scale

The discussion of our results should make clear that there are two levels of interpretation. The first level is the novel, and consistent, young age of CCW rotated strata. The finer (“second-order”) details may be debatable, but do not question the first-order interpretation.

A considerable difficulty when attempting to relate the isotopic ages to the magnetic data is the accuracy, for the time interval of interest, of the existing magnetic polarity time scale (MPTS) (Cande and Kent, 1995). As the latter makes use of very distant tie points, it is clear that the choice of an inaccurate tie point affects a large number of chrons. In the case of the Oligo–Miocene, uncertainties are particularly large because both tie points of relevance to our samples listed in Cande and Kent (1995) MPTS (C5Bn(0.0) at 14.8 Ma, and C6Cn.2r(0.0) at 23.8 Ma) are incorrect (Baksi, 1993; McIntosh et al., 1992; Wei, 1995). According to Cande and Kent (1995) MPTS, revised by Huestis and Acton (1997), our two volcanoclastic levels should fall within Chrons C5Er–C6n. We consider here two important updates for radiometric ages of MPTS tie points: the base of C5Bn.2n is now dated at $16.4 \pm 0.1$ Ma (Baksi, 1993, recalculated for the FCT monitor age of 28.02 Ma (Renne et al., 1998) used in our calculations) and a new integrated age model constrains Chron C6Cn.3n at about 24.2–24.3 Ma (Naish et al., 2001). This latter study provides a precise $^{40}Ar/^{39}Ar$ dating of $24.22 \pm 0.03$ Ma near the base of C6Cn.3n. Therefore, we assumed a calibrated age of 24.250 Ma for the base of C6Cn.3n and performed a simple linear interpolation between the two new tie points. We found that, within the present inherent uncertainties, the samples LV1 and LV2 can be assumed to fall both into Chron C5En (with a revised age of 19.095–19.526 Ma, following calculations described above).

### 9.2. Age of the studied section and of remanence acquisition

The studied strata lack significant fossils, although an early Burdigalian age can be tentatively inferred. The only stringent clues for the section age are given by Ar/Ar dates, yielding $18.94 \pm 0.13$ and $19.20 \pm 0.12$ Ma for the lower (LV1) and upper (LV2) volcanoclastic level, respectively. These Ar/Ar dates indicate an age > 19.1 Ma for the lower part of the section. The two radiometric ages suggest a high sedimentation rate for the lower part of the section (at least), which is consistent with observation of a single normal magnetic polarity in the sequence. Conversely, no age clues are available for the strata located above the volcanic levels.

Our paleomagnetic data show solely normal polarities along all the $\sim 10$ m of studied section, and a rapid shift from about $-20°$ to $0°$ paleodeclination values in the strata above the volcanics, suggestive to represent the CCW rotation of the Corsica–Sardinia block. However, according to our recalculation of chron ages from the Cande and Kent (1995) scale, a normal to reverse transition (C5En–C5Dr) occurred at 19.095 Ma. Therefore, by assuming that the sedimentary sequence is complete and all the sediments were deposited during one normal chron, the CCW rotation would have taken place in < 0.1 Ma, before the transition to the reverse chron. Clearly, this is geologically unreasonable when considering that a large crustal block (both Corsica and Sardinia) rotated.

We conclude that the sedimentary sequence is not complete although the stratigraphic evidence is very ambiguous and a depositional hiatus in the marls between the rotated and unrotated strata is not visible (Fig. 3). However, this stratigraphic interval has reduced susceptibility and remanence, thus reduced detrital input (Fig. 3) and is the most likely candidate to have a lower sedimentation rate and to host sedi-

mentary hiatuses. Another hiatus may also occur further upward, along the disconformity separating the marls from the clays.

The unique normal polarity along the section could also suggest a widespread remagnetization, although not supported by the previously described magnetic characters. However, in order to explain by remagnetization the in situ and tilt-corrected paleomagnetic directions, as well as the CCW rotation in the lower section (Figs. 3 and 7), a complicated process is needed: a first remagnetization, followed by CCW rotation, a further remagnetization of the upper section only, and final strata tilting. We reject this hypothesis as highly unlikely.

In conclusion, the Ar/Ar ages of the two volcanoclastic levels LV1 and LV2 (18.94 ± 0.13 and 19.20 ± 0.12 Ma, respectively) are the only age constraints that we can retain from our study, and the age of the upper part of the section remains a matter of speculation. It may be argued that the upper clays are upper Burdigalian–Langhian, as they seal the small syndepositional extensional faults cutting the marls and the transition from faulted to undeformed sediments in southern Sardinia is known to be late Burdigalian in age (Sowerbutts and Underhill, 1998), but this conclusion remains weak.

### *9.3. Age of the Corsica–Sardinia rotation and Liguro–Provençal Sea spreading*

When compared to the paleodeclination expected for Europe for the lower Burdigalian (at 20 Ma, Besse and Courtillot, in press), the samples below LV2 define a 23.3 ± 4.6° CCW tectonic rotation. Given the inferred sedimentary hiatuses, we cannot constrain the rotation timing, but at least we show that it occurred after 19 Ma (lower–mid Burdigalian), as proved by the Ar/Ar ages. Strike-slip activity is recorded on NE–SW faults cutting all of northern–central Sardinia, but their activity is pre-Burdigalian (Carmignani et al., 1995) and predates the deposition of the sediments studied by us. Therefore, tectonic activity producing locally CCW rotations is not documented in the regional geology, and the paleomagnetic results can be extrapolated to the whole Corsica–Sardinia block (no differential rotation between Corsica and Sardinia was documented by Vigliotti et al., 1990).

A considerable uncertainty still exists on the total amount of the Corsica–Sardinia rotation, as well as on the timing of this event. The old data from Sardinian volcanics (Montigny et al., 1981) seemed to suggest a 30° rotation occurring between 20.5 and 19 Ma, but there is growing evidence that the magnitude of total rotation may be significantly larger, and that the end of the rotation may be 3–4 Ma younger (Todesco and Vigliotti, 1993; Vigliotti and Langenheim, 1995; Muttoni et al., 1998; Gattacceca, 2001; Deino et al., 2001). Our data indicate that Sardinia rotated by 23° after 19 Ma, but cannot help to constrain the amount and timing of the older rotation. By considering the late Burdigalian age of the breakup unconformity observed in Sardinia (Sowerbutts and Underhill, 1998), we argue that the pre-19 Ma rotation occurred during rifting, while the post-19 Ma rotation is likely due to drifting (Fig. 9).

Although our data show that the 23° rotation occurred after 19 Ma and seems to be recorded in less than 1 m of the stratigraphic sequence, the timing of the rotation itself is not clear. However, the oldest possible age for the end of the rotation (i.e. the minimum time span required to complete the rotation) can be estimated considering typical spreading rates in similar back-arc settings. Normally, back-arc basins spread at average speeds of 2–6 cm/year (e.g. Taylor, 1995), although in the Lau Basin (above the Earth's most active zone of mantle seismicity) spreading rates of 6.5–10 cm/year occurred during the Brunhes Chron (Taylor et al., 1996) and up to 16 cm/year are occurring nowadays (Bevis et al., 1995). In the southern Tyrrhenian Sea, an average spreading rate of 6 cm/year and a Messinian apex reaching 8 cm/year were inferred (Patacca et al., 1990). Given these literature values, we believe that it is unlikely that parts of the Liguro–Provençal Basin spread faster than 8 cm/year. By assuming a rotation pole north of Corsica (43.5°N, 9.0°E, Réhault et al., 1984) and the ~ 570 km N–S length of Corsica–Sardinia block undergoing rigid drifting, a ~ 230 km eastward drift of the southern Sardinian edge during the 23° rotation can be calculated. This drift was likely accompanied by the emplacement of oceanic crust in the Liguro–Provençal Basin. A maximum drift rate of 8 cm/year for the southern Sardinian margin implies that the 23° rotation was not completed in less than ~ 3 million years, i.e. at about 16 Ma (early Langhian). This is only a lower

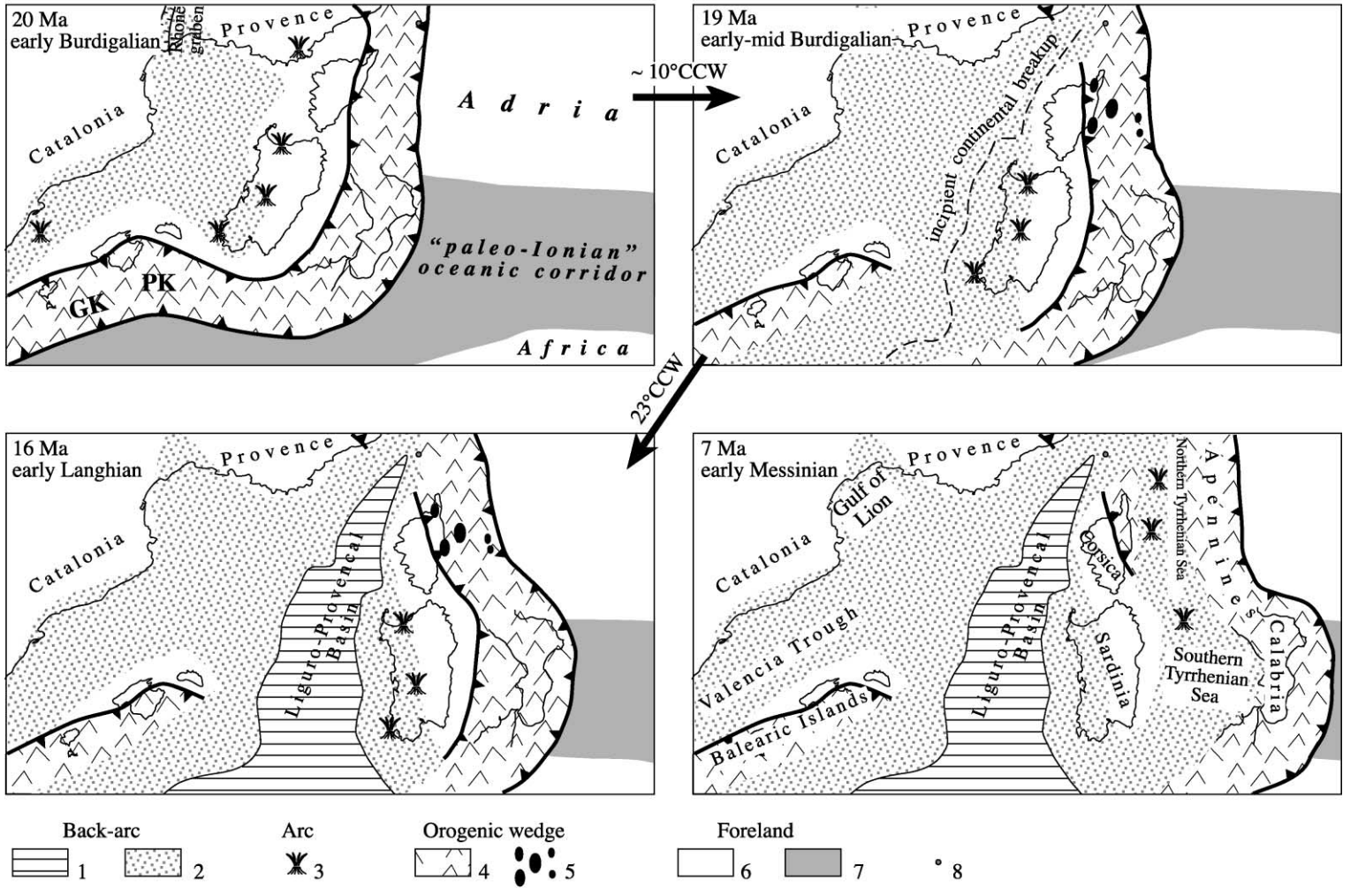


Fig. 9. Inferred tectonic evolution of the central–western Mediterranean from 20 to 7 Ma. The 10° and 23° CCW rotation of the Corsica–Sardinia block occurring during the 20–19 and 19–16 Ma time intervals, respectively, are with respect to Europe held fixed. GK and PK are the Grande Kabylie and Petite Kabylie blocks, respectively. Legend: (1) newly formed oceanic crust; (2) areas affected by rifting; (3) emplacement of arc-related volcanics (or equivalent intrusive rocks) (e.g. Beccaluva et al., 1985; Serri et al., 1993; Lonergan and White, 1997 and references therein); (4) Alpine accretionary wedge; (5) synorogenic "intra-wedge" extensional basins due to local collapse of the overthickened accretionary wedge; (6) continental Adria–Africa lithosphere; (7) oceanic lithosphere of the "paleo-Ionian" Sea; (8) pole for the Corsica–Sardinia rotation (Lat. 43.5°N, Long. 9°E) in present-day coordinates. The ~ 20 Ma Corsica–Sardinia position is inferred from the rotational timing proposed by Gattacceca (2001).

bound for the termination of the rotation, as obviously smaller drift rates would make it even younger. This would imply that the main hiatus(es) should be in the 80–100 cm that record the gradual change from rotated to not-rotated declinations. As a matter of fact, this marl interval has the lowest susceptibility and remanence values (Fig. 3), suggesting a reduced detrital input and sedimentation rate.

Other independent evidence concurs for a ~16–19 Ma age for the Liguro–Provençal oceanic spreading: (1) the upper Burdigalian age of the breakup unconformity observed in Sardinia (Sowerbutts and Underhill, 1998), (2) the 16–17 Ma age of the igneous rocks dredged west of Corsica (Deverchère, 1996; Chamot-Rooke et al., 1999), (3) the high heat flow (>120 mW/m$^2$) in the axial part of the basin, which is the theoretical value for a young oceanic crust (15 Ma according to Chamot-Rooke et al., 1999), and (4) paleomagnetic data from three upper Burdigalian–Langhian (18–15 Ma) sites from Sardinia (Vigliotti and Langenheim, 1995), still showing a small (5–10°) CCW rotation, and recent Ar/Ar dated paleomagnetic directions from a Sardinian volcanic sequence, documenting a 13° rotation occurring after 18.18 ± 0.03 Ma (Deino et al., 2001).

### 9.4. From the Liguro–Provençal to the Tyrrhenian back-arc spreading

The rejuvenation of the Liguro–Provençal Basin spreading and Corsica–Sardinia rotation has significant implications for the timing of the tectonic events in the adjacent Tyrrhenian–Apennine system. It is believed that the Liguro–Provençal and Tyrrhenian seas are both back-arc basins opening in subsequent times west of the same Adriatic/Ionian slab in progressive eastward roll-back (Malinverno and Ryan, 1986). However, the question arises as to why the locus of back-arc spreading migrated eastward during middle–late Miocene, as extension ceased in the Liguro–Provençal domain and jumped east of Corsica–Sardinia, where the Tyrrhenian Sea started to spread.

We propose that the back-arc spreading migration was due to the heterogeneity of the Adriatic/Ionian lithosphere undergoing passive subduction. We estimate that at 16–19 Ma, the lithosphere of a ''paleo-Ionian'' oceanic corridor east of Sardinia (Fig. 9) sunk easily in the mantle causing a speedy trench retreat (and Liguro–Provençal Basin spreading). Faster subduction beneath Sardinia than beneath Corsica, due to the heterogeneous nature of the subducting plate, is a plausible reason to explain the triangular geometry of the Liguro–Provençal Basin and the CCW rotation of Corsica–Sardinia.

At about 16 Ma (according to our model), the Liguro–Provençal basin stopped widening (and Corsica–Sardinia drifting), likely due to the locking of the subduction process as continental lithosphere continued colliding east of Corsica (Fig. 9). Roll-back continued later only along two isolated slab fragments, observed today below the northern and southern Tyrrhenian Sea by seismic tomography (Lucente et al., 1999). From middle–late Miocene onward, only the ''paleo-Ionian'' oceanic corridor underwent rapid passive subduction, generating the southern Tyrrhenian Sea (partly floored by oceanic crust) and the fast Calabrian drift (Malinverno and Ryan, 1986).

Our paleogeographic reconstruction of the nature of the lithosphere subducting in central–western Mediterranean during Tertiary and Quaternary times is supported by data from Serri et al. (1993), who analyzed the characters of the Neogene–Quaternary magmatism of the Tyrrhenian Sea and margins. Serri et al. (1993) argued on petrological–geochemical grounds that the ''paleo-Ionian'' and Adria subduction were oceanic and continental, respectively, and that east of Corsica the transition from oceanic to continental subduction must have occurred in the late Eocene–early Miocene time interval.

### 9.5. Tectonic significance of the lower Miocene northern Tyrrhenian deposits

Our data give a key to interpret the oldest extensional phenomena observed in the northern Tyrrhenian domain. Widespread back-arc extension started in the whole Tyrrhenian domain only since late Tortonian (~8 Ma), as testified by the onset of syn-rift continental sedimentation in several basins from Tuscany (Martini and Sagri, 1993), transgressive continental deposits observed over the western Calabrian margin (Di Nocera et al., 1979) and alluvial fan sequences transgressive over the continental basement drilled east of Sardinia by the ODP Site 654 (Mascle et al.,

1988). Given the clear onset of widespread back-arc extension in the Tyrrhenian realm since late Tortonian, the question arises on the geologic significance of the lower Miocene extensional deposits locally observed in the northern Tyrrhenian Sea and margins that significantly predate the general late Tortonian extension (Jolivet et al., 1990; Carmignani et al., 1995; Mauffret et al., 1999; Cornamusini et al., 2000; Foresi et al., 2000).

We note that our paleogeographic model suggests that the Corsica–Sardinia block did not stop rotating and colliding with the Adriatic lithosphere before ~ 16 Ma or possibly more recently, i.e. well after the onset of the lower Miocene sedimentation in the northern Tyrrhenian Sea (Fig. 9). Clearly, the 19–16 Ma 23° drift-related CCW rotation of Corsica–Sardinia induced strong shortening in the Apennine belt, overthickening the orogenic wedge and inducing tectonic collapses (e.g. Platt, 1986, and references therein). Therefore, the lower Miocene deposits can be interpreted as related to extension developing inside the Apennines wedge (as also proposed by Jolivet et al., 1998), and not as precursors of the northern Tyrrhenian back-arc sediments (as suggested by Bartole, 1995).

## 10. Conclusions

New paleomagnetic and Ar/Ar data from Sardinia show that a 23° CCW rotation of Corsica–Sardinia and contemporaneous Liguro–Provençal Basin spreading occurred after 19 Ma. By considering normal extension rates in other back-arc basins, we infer that the Liguro–Provençal Basin kept spreading (and the Corsica–Sardinia block rotating) for at least 3 million years. Therefore, the rotation is estimated to end not before ~ 16 Ma (early Langhian). A 16–19 Ma age of the Liguro–Provencal Basin, oceanic spreading is consistent with other independent data, such as (1) age of the break-up unconformity observed in Sardinia (Sowerbutts and Underhill, 1998), (2) age of igneous rocks dredged west of Corsica (Deverchère, 1996), (3) elevated heat-flow in the Liguro–Provençal Basin (Chamot-Rooke et al., 1999), and (4) recent paleomagnetic data from Sardinian sediments and volcanics (Vigliotti and Langenheim, 1995; Deino et al., 2001).

## Acknowledgements

We thank C. Faccenna for scientific advice and help in the field during the 1995 sampling campaign, and N. D'Agostino for providing magnificent images of the Liguro–Provençal Basin topography. A.F. Glazner, M. Cosca, G. Ruffet and R. Van der Voo provided thoughtful comments on a preliminary version of the manuscript. We are also grateful to the referees E. Platzman and L. Vigliotti, and the Editor J.-P. Burg for carefully reviewing our paper. This work was partly founded by the European Union project "GeoModAp" (contract EV5V-CT94-0464).

## References

Assorgia, A., Barca, S., Casula, G., Spano, C., 1988. Le successioni sedimentarie e vulcaniche del Miocene nei dintorni di Giave e Cossoine (Logudoro, Sardegna NW). Boll. Soc. Sarda Sci. Nat. 26, 75–107.

Assorgia, A., Barca, S., Rizzo, R., Spano, C., 1992a. The beginning of the Lower Miocene marine sedimentation in western Sardinia (Italy) and its implications with the Oligocene–Miocene rift system. IXth Congress R.C.M.N.S. "Global Events and Neogene Evolution of the Mediterranean" (Barcelona, 1990). Paleontol. Evol. 24–25, 295–305.

Assorgia, A., Barca, S., Spano, C., 1992b. Upper Oligocene–Lower Miocene sequences of the Arbus–Funtanazza Coast (South-Western Sardinia, Italy), IGCP N. 276, Newsletter, 5, 21–31.

Assorgia, A., Barca, S., Spano, C., 1997. A synthesis on the Cenozoic stratigraphic, tectonic and volcanic evolution in Sardinia (Italy). Boll. Soc. Geol. Ital. 116, 407–420.

Baksi, A., 1993. A geomagnetic polarity time scale for the period 0–17 Ma, based on $^{40}Ar/^{39}Ar$ plateau ages for selected field reversals. Geophys. Res. Lett. 20, 1607–1610.

Barca, S., Carmignani, L., Oggiano, G., Pertusati, P.C., Salvadori, I., 1996. Geologic Map of Sardinia, Scale 1:200,000, 2 sheets, Servizio Geologico Nazionale-Regione Autonoma della Sardegna.

Bartole, R., 1995. The north Tyrrhenian–northern Apennines post-collisional system: constraints for a geodynamic model. Terra Nova 7, 7–30.

Bayer, R., Le Mouel, J.-L., Le Pichon, X., 1973. Magnetic anomaly pattern in the western Mediterranean. Earth Planet. Sci. Lett. 49, 168–176.

Beccaluva, L., Civetta, L., Maciotta, G., Ricci, C.A., 1985. Geochronology in Sardinia: results and problems. Rend. Soc. Ital. Mineral. Petrol. 40, 57–72.

Belluso, E., Ruffini, R., Schaller, M., Villa, I.M., 2000. Electron-microscope and Ar isotope characterization of chemically heterogeneous amphiboles from the Palala Shear Zone, Limpopo Belt, South Africa. Eur. J. Mineral. 12, 45–62.

Besse, J., Courtillot, V., in press. Apparent and true polar wander and the geometry of the geomagnetic field in the last 200 million years, J. Geophys. Res.

Bevis, M., Taylor, F.W., Schultz, B.E., et al., 1995. Geodetic observations of very rapid convergence and back-arc extension at the Tonga arc. Nature 374, 249–251.

Blow, W.H., 1967. Late Middle Eocene to Recent planktonic foraminiferal biostratigraphy. Proc. 1st. Intern. Conf. Plankt. Microfossils, Geneve, 1–422.

Burrus, J., 1984. Contribution to a geodynamic synthesis of the Provençal Basin (North-Western Mediterranean). Mar. Geol. 55, 247–269.

Burrus, J., Foucher, J.P., 1986. Contribution to the thermal regime of the Provençal Basin based on flumed heat flow surveys and previous investigations. Tectonophysics 128, 303–334.

Cande, S.C., Kent, D.V., 1995. Revised calibration of the geomagnetic polarity time scale for the Late Cretaceous and Cenozoic. J. Geophys. Res. 100, 6093–6095.

Carmignani, L., Decandia, F.A., Disperati, L., Fantozzi, P.L., Lazzarotto, A., Liotta, D., Oggiano, G., 1995. Relationships between the Tertiary structural evolution of the Corsica–Sardinia–Provençal Domain and the northern Apennines. Terra Nova 7, 128–137.

Chamot-Rooke, N., Gaulier, J.-M., Jestin, F., 1999. Constraints on Moho depth and crustal thickness in the Liguro–Provençal basin from a 3D gravity inversion: geodynamic implications. In: Durand, B., Jolivet, L., Horvath, F., Seranne, M. (Eds.), The Mediterranean Basins: Tertiary Extension Within the Alpine Orogen. Geological Society of London, Special Publications, vol. 156, pp. 37–61.

Cherchi, A., Corradini, D., D'Onofrio, S., Iaccarino, S., Martini, E., Murru, M., Russo, A., 1985. Sardara–Villanovaforru section. In: Cherchi, A. (Ed.), Micropaleontological Researches in Sardinia, 19th European Micropaleontological Colloquium Guidebook, Sardinia October, vol. 1–10, pp. 234–249.

Cornamusini, G., Lazzarotto, A., Merlini, S., Pascucci, V., 2000. Eocene–Quaternary evolution of the Corsica basin-Tuscan shelf area (north Tyrrhenian Sea) through CROP-MARE seismic analysis paper presented at the meeting. Evoluzione geologica e geodinamica dell'Appennino, Foligno (Italy) February 16–18, 108–110 (abstract).

Coulon, C., Demant, A., Bobier, C., 1974. Contribution du paléomagnétisme a l'étude des séries volcaniques cénozoiques et quaternaires de Sardaigne nord-occidentale. Tectonophysics 22, 59–82.

Deino, A., Gattacceca, J., Rizzo, R., Montanari, A., 2001. $^{40}Ar/^{39}Ar$ dating and paleomagnetism of the Miocene volcanic succession of Monte Furru (western Sardinia): implications for the rotation history of the Corsica–Sardinia microplate. Geophys. Res. Lett. 28 (17), 3373–3376.

De Jong, K.A., Manzoni, M., Zijderveld, J.D.A., 1969. Paleomagnetism of the Alghero Trachyandesites. Nature 224, 67–69.

De Jong, K.A., Manzoni, M., Stavenga, T., Van Dijk, F., Van der Voo, R., Zijderveld, J.D.A., 1973. Palaeomagnetic evidence for rotation of Sardinia during the early Miocene. Nature 243, 281–283.

Deverchère, J., et al., 1996. Geodynamics of the Ligurian Basin and Margins, Abstract of the meeting "The Mediterranean Basins", Cergy–Pontoise (Paris, France), December 11–13.

Di Nocera, S., Ortolani, F., Torre, M., Russo, B., 1979. Caratteristiche stratigrafiche e paleoambientali dei depositi altomiocenici nella zona di Falconara Albanese (Catena Costiera Calabra). Boll. Soc. Nat. Napoli 83, 1–29.

Edel, J.B., 1979. Paleomagnetic study of the Tertiary volcanics of Sardinia. J. Geophys. 45, 259–280.

Edel, J.B., Lortscher, A., 1977. Paléomagnétisme du volcanisme tertiaire de Sardaigne. Nouveaux résultats et synthèse. Bull. Soc. Geol. Fr. 19, 815–824.

Farris, M., 1990. Studio geo-vulcanologico e stratigrafico del settore di Monastir–Ussana–Nuraminis, Univ. Cagliari, unpublished thesis, 1–217.

Foresi, L.M., Cornamusini, G., Bossio, A., Ferrandini, M., Mazzei, R., Salvatorini, G., Argenti, P., 2000. The Miocene sedimentary succession of the Pianosa island, northern Tyrrhenian Sea paper presented at the meeting. Evoluzione geologica e geodinamica dell'Appennino, Foligno (Italy) February 16–18, 155–157 (abstract).

Fornaciari, E., Rio, D., 1996. Latest Oligocene to early middle Miocene quantitative calcareous nannofossil biostratigraphy in the Mediterranean region. Micropaleontology 42, 1–36.

Gattacceca, J., 2001. Cinématique du bassin liguro–provencal entre 30 et 12 Ma. Implications géodynamiques, PhD thesis, Ecole des mines de Paris, 299 pp.

Gialanella, P.R., Heller, F., Incoronato, A., 1994. Rock magnetism of deformed upper Triassic limestones from the Lagonegro Basin (southern Apennines Italy). Geophys. Res. Lett. 21, 2665–2668.

Horner, F., Lowrie, W., 1981. Paleomagnetic evidence from Mesozoic carbonate rocks for the rotation of Sardinia. J. Geophys. 49, 11–19.

Huestis, S.P., Acton, G.D., 1997. On the construction of geomagnetic timescales from non-prejudicial treatment of magnetic anomaly data from multiple ridges. Geophys. J. Int. 129, 176–182.

Iaccarino, S., D'Onofrio, S., Murru, M., 1985. Miocene foraminifera of several sections of the Marmilla area (central western Sardinia). Boll. Soc. Paleontol. Ital. 23, 395–412.

Jelinek, V., 1978. Statistical processing of anisotropy of magnetic susceptibility measured on a group of specimens and its applications. Stud. Geophys. Geod. 22, 50–62.

Jolivet, L., Dubois, R., Fournier, M., Goffé, B., Michard, A., Jourdan, C., 1990. Ductile extension in Alpine Corsica. Geology 18, 1007–1010.

Jolivet, L., Faccenna, C., Goffé, B., Mattei, M., Rossetti, F., Brunet, C., Storti, F., Funiciello, R., Cadet, J.-P., D'Agostino, N., Parra, T., 1998. Midcrustal shear zones in postorogenic extension: example from the northern Tyrrhenian Sea. J. Geophys. Res. 103, 12123–12160.

Kastens, K., Mascle, J., Auroux, C., et al., 1986. A microcosm of ocean basin evolution in the Mediterranean. Nature 321, 383–384.

Kirschvink, J.L., 1980. The least-square line and plane and the analysis of paleomagnetic data. Geophys. J. R. Astron. Soc. 62, 699–718.

Lehman, B., Sagnotti, L., Winkler, A., Lo Cascio, C., 1996. Magnetic mineralogy changes in the Pleistocene marine sequence of Montalto di Castro (central Italy) and influences on the magnetic anisotropy. Geophys. J. Int. 127, 529–541.

Lonergan, L., White, N., 1997. Origin of the Betic-Rif mountain belt. Tectonics 16 (3), 504–522.

Lowrie, W., 1990. Identification of ferromagnetic minerals in a rock by coercivity and unblocking temperature properties. Geophys. Res. Lett. 17, 159–162.

Lucente, F.P., Chiarabba, C., Cimini, G.B., Giardini, D., 1999. Tomographic constraints on the geodynamic evolution of the Italian region. J. Geophys. Res. 104, 20307–20327.

Ludwig, K.R., 1999. User's Manual for Isoplot/Ex Version 2.2, A Geochronological Toolkit for Microsoft Excel: Berkeley Geochronology Center Special Publication No. 1a, 53 pp.

Maillard, A., Mauffret, A., Watts, A.B., Torné, M., Pascal, G., Buhl, P., Pinet, B., 1992. Tertiary sedimentary history and structure of the Valencia trough (western Mediterranean). Tectonophysics 203, 57–75.

Malinverno, A., Ryan, W.B.F., 1986. Extension in the Tyrrhenian Sea and shortening in the Apennines as result of arc migration driven by sinking of the lithosphere. Tectonics 5, 227–245.

Manzoni, M., 1974. Un'interpretazione dei dati paleomagnetici del terziario della Sardegna ed alcuni nuovi esempi. Rend. Semin. Fac. Sci. Univ. Cagliari 43, 163–167.

Martini, I.P., Sagri, M., 1993. Tectono-sedimentary characteristics of Late Miocene–Quaternary extensional basins of the northern Apennines, Italy. Earth Sci. Rev. 34, 197–233.

Mascle, J., Kastens, K., Auroux, C., et al., 1988. A land-locked back-arc basin: preliminary results from ODP Leg 107 in the Tyrrhenian Sea. Tectonophysics 146, 149–162.

Mauffret, A., Maillard, A., Pascal, G., Torné, M., Buhl, P., Pinet, B., 1992. Long-listening multichannel seismic profiles in the Valencia trough (Valsis 2) and the Gulf of Lions (ECORS): a comparison. Tectonophysics 203, 285–304.

Mauffret, A., Contrucci, I., Brunet, C., 1999. Structural evolution of the Northern Tyrrhenian Sea from new seismic data. Mar. Pet. Geol. 16, 381–407.

May, S.R., Butler, R.F., Shafiqullah, M., Damon, P.E., 1986. Paleomagnetism of Jurassic rocks in the Patagonia Mountains, southeastern Arizona: implications for the North American 170 Ma reference pole. J. Geophys. Res. 91, 11545–11555.

McFadden, P.L., 1990. A new fold test for paleomagnetic studies. Geophys. J. Int. 103, 163–169.

McIntosh, W.C., Geismann, J.W., Chapin, C.E., Kunk, M.J., Henry, C.D., 1992. Calibration of the latest Eocene–Oligocene geomagnetic polarity time scale using $^{40}Ar/^{39}Ar$ dated ignimbrites. Geology 20, 459–463.

Montigny, R., Edel, J.B., Thuizat, R., 1981. Oligo–Miocene rotation of Sardinia: K–Ar ages and paleomagnetic data of Tertiary volcanics. Earth Planet. Sci. Lett. 54, 261–271.

Muttoni, G., Argnani, A., Kent, D.V., Abrahamsen, N., Cibin, U., 1998. Paleomagnetic evidence for Neogene tectonic rotations in the northern Apennines, Italy. Earth Planet. Sci. Lett. 154, 25–40.

Naish, T.R., Woolfe, K.J., Barrett, P.J., Wilson, G.S., Atkins, C., Bohaty, S.M., Bücker, C.J., Claps, M., Davey, F.J., Dunbar, G., Dunn, A.G., Fielding, C.R., Florindo, F., Hannah, M.J., Harwood, D.M., Watkins, D.K., Henrys, S.A., Krissek, L.A., Lavelle, M., van der Meer, J., McIntosh, W.C., Niessen, F., Passchier, S., Powell, R.D., Roberts, A.P., Sagnotti, L., Scherer, R.P., Strong, C.P., Talarico, F., Verosub, K.L., Villa, G., Wonik, T., 2001. Orbitally induced oscillations in the East Antarctic Ice Sheet at the Oligocene–Miocene boundary. Nature 413, 719–723.

Patacca, E., Sartori, R., Scandone, P., 1990. Tyrrhenian basin and Apenninic arcs: kinematic relations since late Tortonian times. Mem. Soc. Geol. Ital. 45, 425–451.

Pecorini, G., Pomesano Cherchi, A., 1969. Ricerche geologiche e biostratigrafiche sul Campidano meridionale (Sardegna). Mem. Soc. Geol. Ital. 8, 421–451.

Platt, J.P., 1986. Dynamic of orogenic wedges and the uplift of high-pressure metamorphic rocks. Geol. Soc. Am. Bull. 97, 1037–1053.

Réhault, J.-P., Boillot, G., Mauffret, A., 1984. The western Mediterranean basin geological evolution. Mar. Geol. 55, 447–477.

Renne, P.R., Swisher, C.C., Deino, A.L., Karner, D.B., Owens, T.L., DePaolo, D.J., 1998. Intercalibration of standards, absolute ages and uncertainties in $^{40}Ar/^{39}Ar$ dating. Chem. Geol. 145, 117–152.

Sagnotti, L., Speranza, F., Winkler, A., Mattei, M., Funiciello, R., 1998. Magnetic fabric of clay sediments from the external northern Apennines (Italy). Phys. Earth Planet. Inter. 105, 73–93.

Sartori, R., 1989. Evoluzione neogenico–recente del bacino tirrenico e suoi rapporti con la geologia delle aree circostanti. G. Geol. 3 (51/2), 1–39.

Serri, G., Innocenti, F., Manetti, P., 1993. Geochemical and petrological evidence of the subduction of delaminated Adriatic continental lithosphere in the genesis of the Neogene–Quaternary magmatism of central Italy. Tectonophysics 223, 117–147.

Smith, J.V., 1974. Feldspar Minerals, vol. 2. Springer, Berlin, 690 pp.

Sowerbutts, A.A., Underhill, J.R., 1998. Sedimentary response to intra-arc extension: controls on Oligo–Miocene deposition, Sarcidano sub-basin, Sardinia. J. Geol. Soc. (London) 155, 491–508.

Taylor, B. (Ed.), 1995. Backarc Basins, Tectonics and Magmatism. Plenum, New York, 524 pp.

Taylor, B., Zellmer, K., Martinez, F., Goodliffe, A., 1996. Sea-floor spreading in the Lau back-arc basin. Earth Planet. Sci. Lett. 144, 35–40.

Todesco, M., Vigliotti, L., 1993. When did Sardinia rotate? Statistical evaluation of the paleomagnetic data. Ann. Geofis. 36, 119–134.

Van der Voo, R., 1993. Paleomagnetism of the Atlantic, Thethys, and Iapetus Oceans. Cambridge Univ. Press, Cambridge, 411 pp.

Vigliotti, L., Langenheim, V.E., 1995. When did Sardinia stop rotating? New paleomagnetic results. Terra Nova 7, 424–435.

Vigliotti, L., Alvarez, W., Mc Williams, M., 1990. No relative motion detected between Corsica and Sardinia. Earth Planet. Sci. Lett. 98, 313–318.

Villa, I.M., Hermann, J., Müntener, O., Trommsdorff, V., 2000. $^{39}Ar–^{40}Ar$ dating of multiply zoned amphibole generations

(Malenco, Italian Alps). Contrib. Mineral. Petrol. 140, 363–381.
Wei, W., 1995. Revised age calibration points for the geomagnetic polarity time scale. Geophys. Res. Lett. 22 (8), 957–960.
Westphal, M., Orsini, J., Vellutini, P., 1976. Le microcontinent corso-sarde, sa position initiale: données paléomagnétiques et raccords géologiques. Tectonophysics 30, 141–157.
Zijderveld, J.D.A., De Jong, K.A., Van der Voo, R., 1970. Rotation of Sardinia: palaeomagnetic evidence from Permian rocks. Nature 226, 933–934.